

Electromagnetic Probes and Heavy Flavor in PHENIX

Deepali Sharma (For the PHENIX Collaboration)

Department of Particle Physics, The Weizmann Institute of Science, Rehovot, 76100, Israel

Abstract

These proceedings summarize the di-electron spectrum measurements by PHENIX in $p + p$ and $Au + Au$ collisions at $\sqrt{s_{NN}} = 200$ GeV, along with a comparison to the expectations from hadronic sources and various model predictions. An overview of the latest PHENIX results on open heavy flavor and quarkonia production, measured through the electron and muon channels at mid-rapidity and forward/backward rapidity for $p + p$, $d + Au$ and $Au + Au$ collisions is also presented.

Key words: Quark gluon plasma, heavy quarkonium, open heavy flavor, dileptons

Electromagnetic probes such as dileptons and photons are ideal for the investigation of the hot and dense matter created in high energy heavy ion collisions. Being colorless, they do not suffer any strong interaction, and so carry all the information about the conditions and properties at the time of their production. The dilepton pairs originate either from the pseudo-scalar or vector-meson decays, typically after the collision, or from hard scattering processes like open heavy flavor production, Drell-Yan pair production *etc*, all occurring early in the collision. The measurement of direct thermal radiation (photons or dileptons) can be used to derive a limit on the initial temperature of the hot and dense medium created in the heavy ion collisions

The PHENIX detector [1] at RHIC has measured dileptons in $p + p$ and $Au + Au$ collisions at mid-rapidity. The heavy flavor has been measured using non-photonic electrons at mid-rapidity ($|\eta| \leq 0.35$) and muons at forward rapidity ($1.2 \leq \eta \leq 2.4$). Charmonium has been measured in different states (J/ψ , ψ' and χ_c) by fully reconstructed leptonic decays (e^+e^-) at mid and forward/backward ($\mu^+\mu^-$) rapidity. The following sections report these measurements for $p + p$, $d + Au$ and $Au + Au$ collisions at $\sqrt{s_{NN}} = 200$ GeV and what is expected for the near future.

1. Low mass dileptons

PHENIX has measured the e^+e^- mass spectrum in $p + p$ [2] and $Au + Au$ [3] collisions at $\sqrt{s_{NN}} = 200$ GeV as a function of transverse momentum and mass. Fig. 1 shows the invariant mass distribution of electron pairs measured in $p + p$ (left) and minimum bias $Au + Au$ (right) collisions. The combinatorial background was subtracted statistically utilizing mixed events and the like-sign pairs. The data are compared to a cocktail of the expected hadronic sources calculated using a Monte Carlo and filtered by the PHENIX acceptance. For $p + p$ collisions, the agreement between data and simulation over the full mass range of $0 < m_{ee} < 8$ GeV/ c^2 is excellent, as is evident from the ratio of data to cocktail shown in the lower left panel. A comparison of the integrated yield between data and PYTHIA in the intermediate mass region of $1.1 < m_{ee} < 2.5$ GeV/ c^2 , which is dominated by open charm, yielded a total charm cross-section of $\sigma_{c\bar{c}} = 544 \pm 39(\text{stat.}) \pm 142(\text{syst.}) \pm 200(\text{model}) \mu\text{b}$ in the $p + p$ collisions. Using a simultaneous fit of the mass shapes from simulation to the data, the charm and bottom cross-sections were disentangled. The fit results yielded $\sigma_{c\bar{c}} = 518 \pm 47(\text{stat.}) \pm 135(\text{syst.}) \pm 190(\text{model}) \mu\text{b}$ and $\sigma_{b\bar{b}} = 3.9 \pm 2.4(\text{stat.}) \pm 3.2(\text{syst.}) \mu\text{b}$ respectively, for the charm and bottom cross-sections.

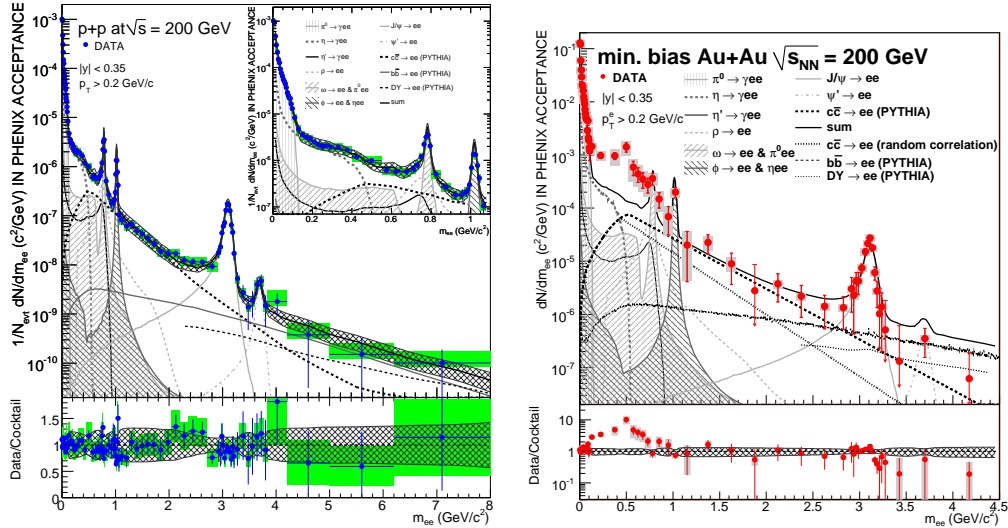


Fig. 1. Electron-positron pair yield per inelastic collision as a function of pair mass in $p + p$ (left) and $Au + Au$ (right). The data are compared to a cocktail of known sources.

The right panel in Fig. 1 shows the e^+e^- pairs measured in minimum bias $Au + Au$ collisions, after subtracting the combinatorial background. An excellent agreement to the cocktail is seen at very low masses, up to ~ 100 MeV/ c^2 . For the masses above the ϕ meson, the agreement is also good, in particular the continuum in the intermediate mass region is fully accounted by the contribution from charm decays. However, in the low mass region from $0.15 \leq m_{e^+e^-} \leq 0.75$ GeV/ c^2 , there is a considerable excess of e^+e^- pairs of the order of $3.4 \pm 0.2(\text{stat.}) \pm 1.3(\text{syst.}) \pm 0.7(\text{model}) \mu\text{b}$. The excess is present at all pair p_T , but is more pronounced at low pair p_T ($p_T < 0.7$ GeV/ c) [3].

The enhancement was also studied as a function of centrality. The integrated yield, divided by the number of participating nucleons pairs ($N_{part}/2$) is shown in the left and middle panels of Fig. 2 for three different mass windows. Whereas the low mass yield for the region dominated by π^0 Dalitz decay ($0 < m_{ee} < 100 \text{ MeV}/c^2$), is in good agreement with the cocktail (left panel (b)), reflecting the expected increase with the pion yield, a very strong enhancement is observed in the low mass continuum region ($150 < m_{ee} < 750 \text{ MeV}/c^2$). The yield in the mass region, $1.2 < m_{ee} < 2.8 \text{ GeV}/c^2$ normalized to the number of binary collisions (middle panel Fig. 2) shows no significant centrality dependence and is consistent with the expectations based on PYTHIA. However, this scaling with N_{coll} which is expected for charmed meson decays [4], may be a mere coincidence resulting from two balancing effects: the suppression of charm which increases with N_{part} and a thermal contribution that could increase faster than linearly with N_{part} . So far, the models that successfully described the low mass region results at SPS based on the broadening of the ρ meson spectral function, fail to reproduce PHENIX results [10, 11] as can be seen in the right panel of Fig. 2.

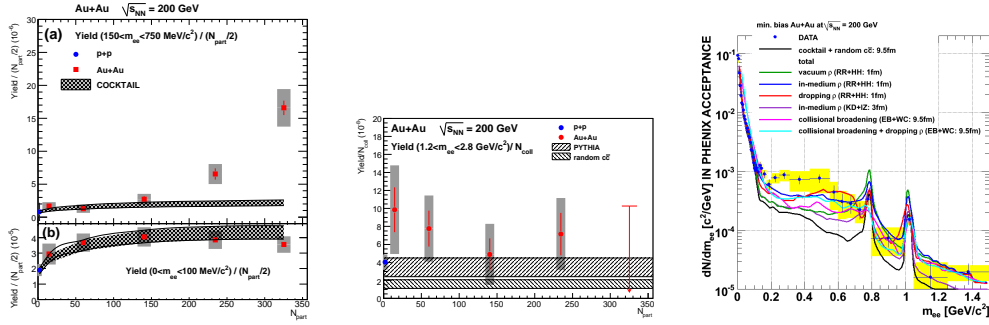


Fig. 2. Integrated yield per pair of participating nucleons as a function of N_{part} compared to the expectations for three different mass slices (Left and middle panels). Right: Comparison of $Au + Au$ data to various models that successfully describe data from lower energies.

Utilizing the idea that every source of real photons should also emit virtual photons which convert to low mass e^+e^- pairs, PHENIX analyzed the dilepton yield observed in $Au + Au$ collisions with low masses ($m_{ee} < 300 \text{ MeV}/c^2$) and high transverse momentum ($1 < p_T < 5 \text{ GeV}/c$). In this restricted kinematic window, PHENIX observes a significant excess of e^+e^- pairs beyond the expected yield from the hadronic cocktail of light mesons and open charm decays as seen in Fig. 3. The e^+e^- invariant mass excess is transformed into a spectrum of real photons under the assumption that the excess is entirely due to internal conversion of photons. Fig. 3 (right panel) shows the resulting invariant cross-section for the direct photons. The figure also shows the direct photon data measured by PHENIX at high p_T in $Au + Au$ collisions [3, 5]. The two data sets are in good agreement over the p_T region of overlap. The $p + p$ data shown in the figure is very well described by NLO pQCD direct photon calculations (solid lines on the $p + p$ data) and by a power-law fit (dashed lines). The $Au + Au$ data on the other hand, are clearly above the $p + p$ fit scaled by nuclear overlap function T_{AA} (dashed lines). The $Au + Au$ data is fitted using the T_{AA} scaled power law fit to $p + p$ plus an exponential (solid lines). The exponential part of the fit yields an inverse slope parameter of $T = 221 \pm 19(stat.) \pm 19(syst.) \text{ MeV}$ in the central collisions, and within errors is independent of the centrality. Interpreted as thermal radiation, this would represent the temperature of the system averaged over

the space-time evolution of the collision. According to hydrodynamical models, this corresponds to an initial temperature of $T_i = 300(600)$ MeV for a thermalization time of 0.6 (0.15) fm/c [6].

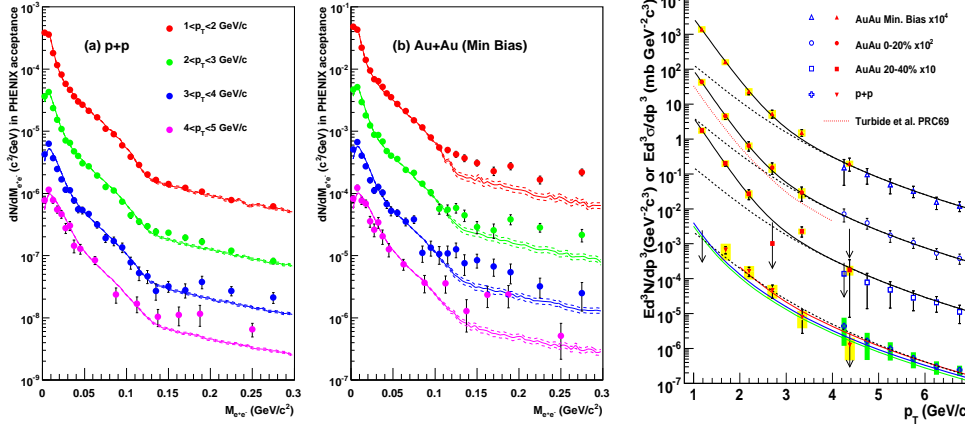


Fig. 3. The e^+e^- invariant mass distributions in (a) $p+p$ and (b) minimum bias $Au+Au$ collisions compared to a cocktail of hadronic sources. Invariant cross-section ($p+p$) and invariant yield (au) of direct photons compared to a NLO pQCD calculation (red, green, blue curve). The black curves are exponential plus modified power-law fit [3].

2. Open heavy flavor

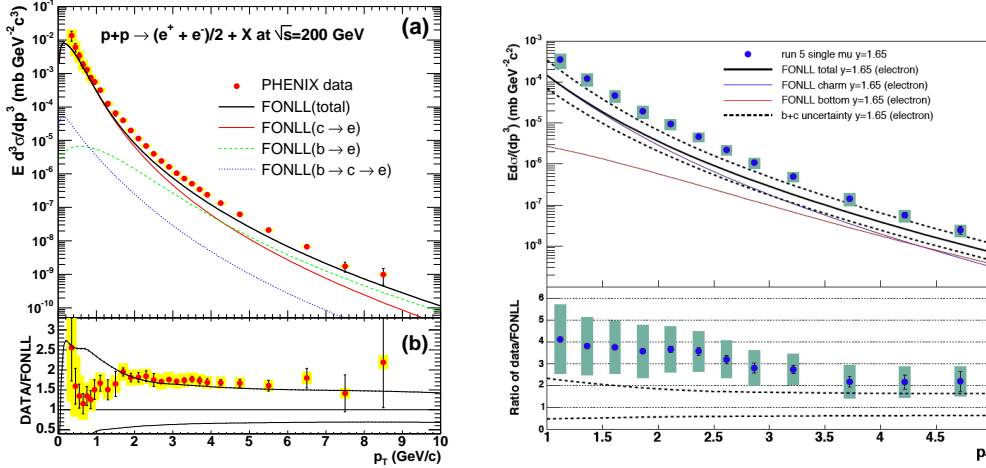


Fig. 4. Invariant differential cross-section of electrons (left) at $\langle y \rangle = 0$, and muons at $\langle y \rangle = 1.65$ (right) from the heavy flavor decays. The curves are the FONLL calculations.

PHENIX measures open heavy flavor indirectly via the semi-leptonic decays [7]. The inclusive electron spectrum consists of the following three components: (1) electrons

from heavy flavor decays, (2) “photonic” background electrons from Dalitz decays of light mesons and photon conversions mainly in the beam pipe, and (3) “non-photonic” background electrons from the K_{e3} decays and dielectron decays of vector mesons. The heavy flavor electron spectrum is obtained by subtracting the background components from the inclusive spectrum using two independent and complementary methods. The first method is known as “Cocktail method”, where a cocktail of electron spectra from various background sources is calculated using a Monte Carlo event generator and subtracted from the inclusive spectrum. The most important background is the π^0 Dalitz decay and γ -conversions, and so we use our measured π^0 and π^\pm spectra as input to the generator. The results are cross-checked by a complementary method referred to as “Converter method”, where we add a known amount of material in the detector acceptance and measure how the production of single electrons is affected.

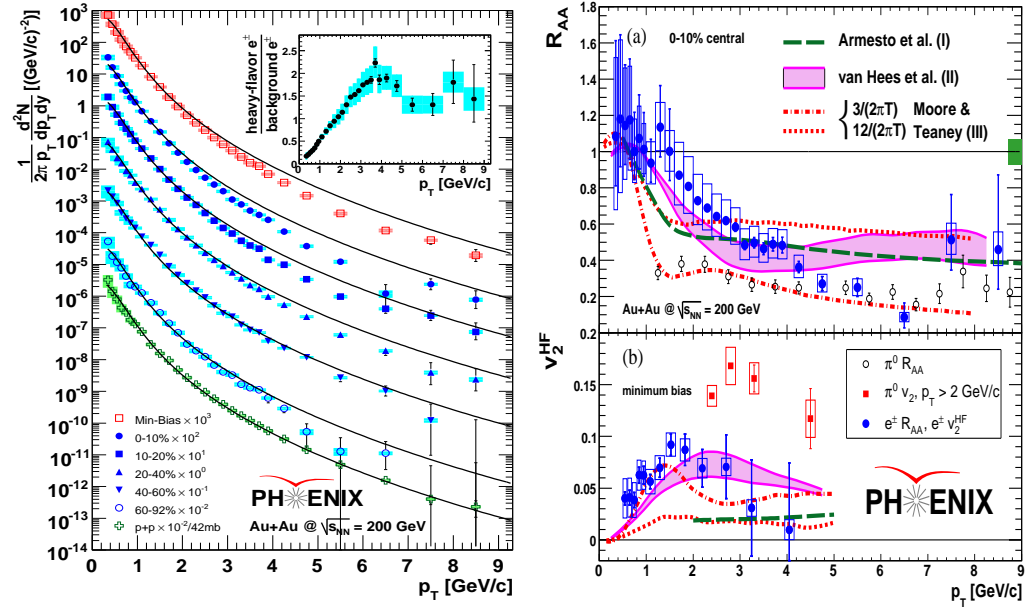


Fig. 5. Left: Invariant yields of electrons from heavy flavor for different $Au + Au$ centrality classes and $p + p$, plotted together with N_{coll} scaled $p + p$ FONLL calculations (solid lines). The insert shows the ratio of heavy flavor to background electrons for minimum bias $Au + Au$ collisions. Right: (a) R_{AA} of heavy flavor electrons in 0-10% central collisions with π^0 data and model calculations. The box at $R_{AA} = 1$ shows the uncertainty in T_{AA} . (b) v_2^{HF} of heavy flavor electrons in minimum bias collisions compared with the π^0 data.

The left panel in Fig. 4 shows the spectrum of electrons from heavy flavor in $p + p$ collisions, along with Fixed Order plus Next-to-Leading-Log pQCD (FONLL) predictions. The bottom panel shows the ratio of the data to the FONLL calculations, which is nearly p_T independent over the entire p_T range. The total charm cross-section obtained from the non-photonic electron spectrum is $\sigma_{c\bar{c}} = 567 \pm 57(stat.) \pm 193(syst.)$. Similar measurements were performed for single muons at $\langle y \rangle = 1.65$, in which the background cocktail approach is used. Single muons were measured in both forward and backward directions and the combined spectrum is shown in the right panel of Fig. 4 along with

FONLL predictions [8]. The yield at forward rapidity agrees with FONLL for $p_T > 3.5$ GeV/c, where the S/B is better.

In $Au + Au$ collisions, electrons from heavy flavor were measured following the same techniques as in $p + p$ collisions. The left panel in Fig. 5 [9] shows the invariant p_T spectra of electrons from heavy flavor decay for minimum bias and various centrality classes. The curves overlayed are the fit to the corresponding data for $p + p$ collisions, with the spectral shape taken from the FONLL calculation and scaled by the nuclear overlap integral $\langle T_{AA} \rangle$ for each centrality class. For all the centralities, the $Au + Au$ spectra agree well with the $p + p$ reference at low p_T , but a suppression with respect to $p + p$ can be seen at high p_T . This can be expressed quantitatively in terms of the nuclear modification factor R_{AA} , which is defined as the ratio of the yield in $Au + Au$ collisions to the yield in $p + p$ collisions, normalized by the number of binary collisions. The top right panel in Fig. 5 shows the R_{AA} of heavy flavor electrons for the 10% most central $Au + Au$ collisions, plotted along with π^0 results. At intermediate p_T , the suppression is compatible with the scenario of larger energy loss for the lighter quarks, but for $p_T > 4.0$ GeV, the suppression level is almost the same as that of π^0 . The $Au + Au$ data thus indicate a strong coupling of heavy quark to the medium, as is evident from the bottom right panel of Fig. 5, which shows a non-negligible v_2 for the heavy flavor electrons.

3. Quarkonia

PHENIX has measured J/ψ , ψ' and Υ in $p + p$ collisions [12–14], as well as J/ψ and Υ in $Au + Au$ collisions [14, 15]. The rapidity and p_T distributions of J/ψ produced in $p + p$ collisions are shown in Fig. 6, along with some theoretical calculations [13]. The J/ψ measurements include feed-down from excited states, namely ψ' , χ_c and Υ . PHENIX has preliminary yield ratio measurements of these particles at mid-rapidity. The results show that about $8.6 \pm 2.5\%$ are from ψ' and up to 42% (90% CL) are from χ_c .

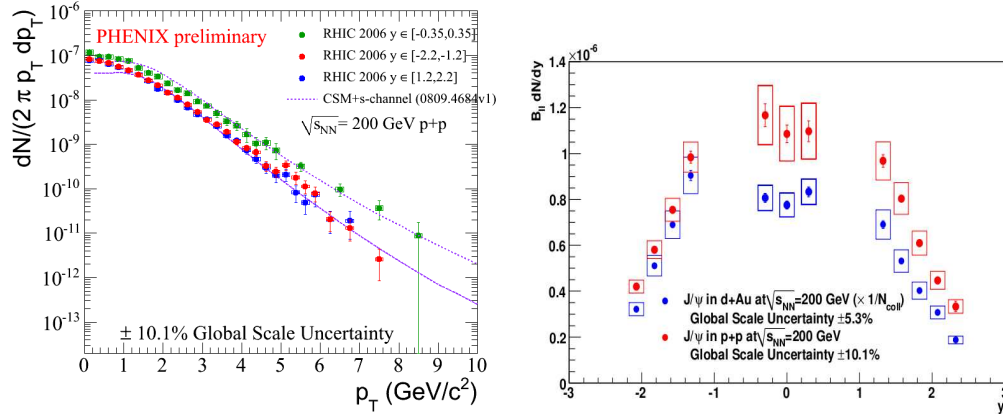


Fig. 6. J/ψ cross-section as a function of p_T (left) and rapidity (right) in $p + p$ collisions.

The R_{AA} results of PHENIX, plotted as a function of number of participating nucleons (N_{part}), in $Cu + Cu$ and $Au + Au$ collisions [15, 16] are shown in the left panel of Fig. 7. The two data sets are in good agreement with each other about the dependence of

the nuclear modification on N_{part} , with $Cu + Cu$ data defining the dependence better at low N_{part} . Results on the p_T dependence can be found in [15, 16], which are of considerable theoretical interest as being the signature of suppression mechanism. In $Au + Au$ collisions, PHENIX observed a suppression substantially stronger at forward rapidity as compared to the suppression at mid-rapidity, referred to as J/ψ suppression puzzle, as can be seen in the bottom left panel of Fig. 7. On the other hand, the NA50 results for $Pb + Pb$ collisions at $\sqrt{s_{NN}} = 17.3$ GeV [17] show a suppression at $y \approx 0.5$, which is comparable to the PHENIX mid-rapidity results. Recently, PHENIX has made progress in understanding these observations from the studies of cold nuclear matter (CNM) effects.

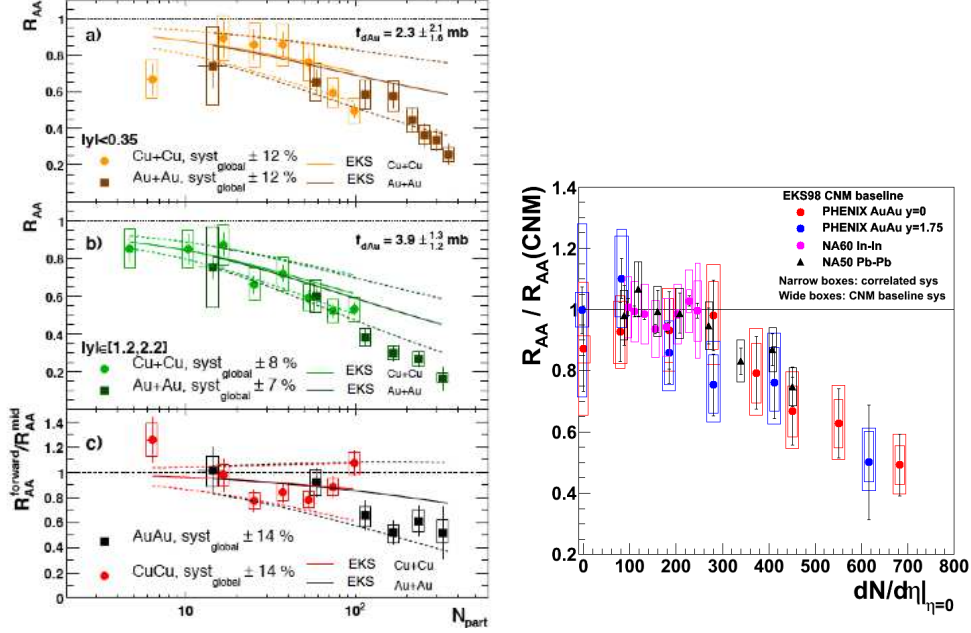


Fig. 7. (a),(b) The nuclear modification factor, R_{AA} for $Cu + Cu$ and $Au + Au$ collisions as a function of N_{part} . (c) Ratio of the forward/backward rapidity to mid-rapidity R_{AA} values. Right panel: The ratio of measured R_{AA} to estimated $R_{AA}(CNM)$ vs N_{part} .

PHENIX collected a high yield $d + Au$ data set during 2008 RHIC run. Results of the final analysis of this data set, that show the yield ratio between the central and peripheral collisions *i.e.* R_{cp} , and R_{dA} have been released [18, 19]. Attempts have been made to describe the integrated R_{cp} as a function of rapidity using the Color Evaporation Model (CEM) that includes EKS98 shadowing plus a fitted breakup cross-section for each rapidity interval (for details see [19, 21]). The fit results are then used to estimate the CNM contributions to the $Au + Au$ R_{AA} data [20]. Using these calculations, the differences between mid and forward rapidity are washed out as can be seen in the right panel of Fig. 7, which shows ratio of the measured R_{AA} to the estimated $R_{AA}(CNM)$. The remaining similar suppression observed at forward and mid rapidity presumably reflects the effects of the final state in $Au + Au$ collisions. Studies are underway to explore the p_T dependence of the suppression as a function of rapidity.

4. Outlook

In 2010 RHIC run, PHENIX collected large $Au + Au$ data sets at $\sqrt{s_{NN}} = 200, 62.4$ and 39 GeV, with a new Hadron Blind Detector (HBD) [22, 23]. HBD is a windowless Čerenkov detector that uses CF_4 as both radiator and active gas. HBD will allow to have better precision measurements for the low mass dielectron measurements by reducing the combinatorial background. These data sets are currently being analyzed. Analysis of the $d + Au$ data is also ongoing, that will allow us to identify cold nuclear matter effects.

PHENIX has now installed a new vertex detector (VTX) [24], which consists of a silicon pixel and silicon strip barrel that is designed to measure displaced vertices from heavy flavor decays. A FVTX detector [25] having the same acceptance as PHENIX muon arms will be added in 2012. These silicon detectors will provide the capability to cleanly separate charm and bottom semileptonic decays, providing for the first time at RHIC, precise measurements of the charm and bottom suppression. The displaced vertex quality will allow to measure the J/ψ cross-section due to bottom quark decays. This will be an important input for studying the J/ψ suppression at high p_T , once the RHIC luminosity upgrade is completed for the 2013 run. The FVTX will also allow the mass separation of J/ψ and ψ' at forward rapidity.

References

- [1] K. Adcox *et.al.*, Nucl. Instrum. Meth. A499 (2003) 469.
- [2] A. Adare *et.al.*(PHENIX), Phys. Lett. B670 (2009) 313.
- [3] A. Adare *et.al.*(PHENIX), Phys. Rev. C81 (2010) 034911.
- [4] A. Adare *et.al.*, Phys. Rev. Lett. 97, 252002 (2006)
- [5] A. Adare *et.al.*(PHENIX), Phys. Rev. Lett. 98 (2007) 012002.
- [6] D. d'Enterria and D. Peressounko, Eur. Phys. J. C46 (2006).
- [7] A. Adare *et.al.*, Phys. Rev. Lett. 97, (2006) 252002.
- [8] D. Hornback, Jour. Phys. G: Nucl. Part. Phys.35,(2008) 104113 (5pp).
- [9] A. Adare *et.al.*, Phys. Rev. Lett. 98, (2007) 172301.
- [10] E.L. Bratkovskaya, W. Cassing and O.Linnyk, Phys. Lett. B670, (2009) 428
- [11] K. Dusling and I. Zahed, arXiv:0712.1982 [nucl-th].
- [12] A. Adare *et.al.*, Phys. Rev. Lett. 98, (2007) 232002.
- [13] C. L. da Silva, Nucl. Phys. A830 (2009) 227c.
- [14] E. T. Atmossa, Nucl. Phys. A830 (2009) 331c.
- [15] A. Adare *et.al.*, Phys. Rev. Lett. 98, (2007) 232301.
- [16] A. Adare *et.al.*, Phys. Rev. Lett. 101, (2008) 122301.
- [17] B. Alessandro, *et.al.*, Eur. Phys. J. C39 (2005) 335.
- [18] L. A. Linden Levy, Nucl. Phys. A830 (2009) 353c.
- [19] A. Adare *et.al.*, arXiv:1010.1246.
- [20] N. Brambilla, *et.al.*, arXiv:1010.5827.
- [21] J. L. Nagle *et.al.*, arXiv:1011.4534.
- [22] I. Ravinovich, Nucl. Phys. A774, (2006) 903.
- [23] Nucl. Instrum. Meth. A523, (2004) 345.
- [24] R. Nouicer, POS (Vertex 2007) 042.
- [25] J. S. Kapustinsky, Nucl. Instrum. Meth. A617 (2010) 546.